

Research Article

Zhongyang Xu, Ningyu Xu, Tingcui Zhang, Jing Wang, Xiaoqi Wang*

Cardioprotective effects of nanoparticles green formulated by *Spinacia oleracea* extract on isoproterenol-induced myocardial infarction in mice by the determination of PPAR- γ /NF- κ B pathway

<https://doi.org/10.1515/chem-2024-0058>

received April 15, 2024; accepted June 1, 2024

Abstract: We developed a contemporary cardioprotective medication using silver nanoparticles (AgNPs) loaded with *Spinacia oleracea* to treat isoproterenol (ISO)-induced myocardial infarction in mice, focusing on the PPAR- γ /NF- κ B pathway. The physicochemical techniques, such as Fourier-transform infrared spectroscopy, field emission scanning electron microscopy, ultraviolet–visible spectroscopy, and energy dispersive X-ray analysis, were employed to characterize the AgNPs. In the *in vivo* experiment, myocardial infarction was induced in mice by administering ISO subcutaneously at a dose of 40 mg/kg every 12 h for a total of three times. The mice were divided into five groups in a random manner: (1 and 2) ISO + AgNPs at varying doses (10 and 20 μ g/mL) and time points; (3) ISO; and (4) control. Following the treatment, cardiac function was assessed through electrocardiogram, as well as biochemical and histochemical analyses. In the study, we examined the inflammatory reactions and cell death in human coronary artery endothelial cells exposed to lipopolysaccharide (LPS). The PPAR- γ /NF- κ B activation by LPS

and the resulting cytokine production were checked using real-time PCR and western blot techniques. The typical ST segment depression in myocardial infarction mice is significantly inhibited by the administration of AgNPs. Additionally, the treatment with AgNPs leads to a significant improvement in ventricular wall infarction, a decrease in mortality rate, and inhibition of myocardial injury marker levels. Furthermore, the application of AgNPs resulted in a decrease in the inflammatory environment within the hearts of mice with myocardial infarction. This effectively prevented the increase in TNF- α , IL-1 β , and IL-6. The gene expression normalization of PPAR- γ /NF- κ B/I κ B- α /IKK α / β and PPAR- γ phosphorylation could potentially be linked to the advantageous impacts of AgNPs. In the context of an *in vitro* experiment, the administration of AgNPs demonstrated a notable decrease in cell death and inflammation cytokines expression inhibition. The myocardial infarction mice in the pre + post-ISO group appear to experience more noticeable cardioprotective effects from the treatment with AgNPs than those in the post-ISO group. Our research findings demonstrate that AgNPs possess cardioprotective efficacies in ISO-induced myocardial infarction. This beneficial effect may be attributed to the PPAR- γ activation and the NF- κ B signaling inhibition. Consequently, our study presents a novel remedial approach for myocardial infarction treatment in clinical settings.

Keywords: myocardial infarction, NF- κ B, PPAR- γ , silver nanoparticles, *Spinacia oleracea*

* **Corresponding author: Xiaoqi Wang**, Department of Cardiovascular, Jinan Central Hospital, Shandong University, No. 105, Jiefang Road, Jinan, Shandong, 250013, China; Department of Cardiovascular, Central Hospital Affiliated to Shandong First Medical University, No. 105, Jiefang Road, Jinan, Shandong, 250013, China, e-mail: qiqi.86@126.com, qiqi.86@outlook.com

Zhongyang Xu: Department of Cardiovascular, Jinan Central Hospital, Shandong University, No. 105, Jiefang Road, Jinan, Shandong, 250013, China; Department of Cardiovascular, Central Hospital Affiliated to Shandong First Medical University, No. 105, Jiefang Road, Jinan, Shandong, 250013, China

Ningyu Xu, Tingcui Zhang, Jing Wang: Department of Cardiovascular, Central Hospital Affiliated to Shandong First Medical University, No. 105, Jiefang Road, Jinan, Shandong, 250013, China

1 Introduction

Myocardial infarction, also known as a heart attack, is the most fatal form of ischemic heart disease globally [1,2]. The global population affected by this condition amounts to approximately 3,000,000 individuals, with nearly half of

all deaths caused by cardiovascular diseases being attributed to myocardial infarction [1–3]. Insufficient flow of oxygen-rich blood through the coronary artery can result in an imbalance in oxygen levels, ultimately causing damage to the heart tissue [2,4]. Effective management of acute myocardial infarction relies heavily on promptly restoring blood flow to the heart. At present, the most successful approaches for achieving this are thrombolytic therapy and percutaneous coronary intervention. Nevertheless, while this technique saves lives, it can also result in the demise of myocardial cells and the impairment of heart function. Numerous studies have indicated that many biochemical and pathophysiological factors contribute to myocardial infarction occurrence [1,5,6]. Nevertheless, the etiology and pathophysiology of myocardial infarction remain uncertain. Furthermore, the existing approach to treat myocardial infarction is constrained by diverse adverse effects including elevated blood pressure, gastrointestinal disorders, and heartburn [7–9]. It is crucial to discover natural compounds that possess anti-apoptotic, antioxidant, and anti-inflammatory properties to reduce damage to the heart tissue or provide protection [10–12].

Nanoparticles have garnered attention because of their significance in biology and their potential applications in medicine. However, the conventional chemical methods employed in their production often lead to the inclusion of hazardous reactive substances, rendering the resulting nanoparticles inappropriate for medical purposes. Using the green approach in nanoparticle synthesis has been widely recognized in various research papers [4–6], resulting in its establishment as a prominent area of interest. Plant extracts are emerging as a promising alternative to traditional ways of yielding metal oxide NPs [7–9]. Nanoparticles exhibit considerable potential in the field of therapy, as they possess the ability to selectively target abnormal tissues or patient cells through active or passive targeting [9,11]. This presents a promising treatment alternative for a range of diseases. Various strategies involving nanoparticles have been developed, focusing on tumor heterogeneity and stroma, offering valuable insights to healthcare professionals and experts in nanotechnology for developing targeted therapies for abnormal cells [10–12]. Recognizing and addressing the limitations and challenges of utilizing NPs in therapy [8–11] holds significant significance. Challenges encompass concerns regarding production and compliance, disparities in nanoparticle characteristics, improvements in permeability and retention, constraints in load-bearing capacity, and physiological barriers [9–12].

Silver nanoparticles (AgNPs) are viral among metal nanoparticles and are extensively utilized in biomedical products due to their wide-ranging antimicrobial properties [13]. AgNPs have recently been found to possess antioxidant properties [14–16], with the balance between antioxidant

and pro-oxidant effects being influenced by the choice of coating agent during AgNPs preparation [16]. It is worth mentioning that AgNPs also exhibited anti-inflammatory characteristics [15–17] through the initiation of M1 macrophage apoptosis and the M1-to-M2 macrophage repolarization [18–20]. Several *in vivo* investigations have documented the potential efficacy of AgNPs in treating inflammatory conditions. For instance, AgNPs have shown promising results in reducing symptoms of collagen-induced rheumatoid arthritis [18], facilitating alloxan-induced diabetes in mice [21], countering diethyl nitrosamine-induced hepatocarcinogenesis in mice [20], mitigating streptozotocin-induced hepatotoxicity in rats [19], managing dextran sodium sulfate-induced colitis in mice [17], and alleviating neuropathy in diabetic rats [15]. Despite the therapeutic benefits of AgNPs, their use has been linked to various toxicology concerns including cell death, immunological response, autophagy, mitochondrial dysfunction, and cytotoxicity [22–24]. Consequently, developing a modern AgNP formulation that minimizes side effects poses a significant challenge. Previous studies have suggested using the AgNPs as novel cardioprotective supplements or drugs [2,5,9]. Arozal et al. indicated the protective efficacies of AgNPs in myocardial infarction induced by isoproterenol (ISO) in rats [2].

Within this research, we focus on developing environmentally friendly AgNPs utilizing *Spinacia oleracea*. The AgNPs underwent examination through microscopic imaging, diffraction, and spectroscopic analysis to comprehend their size, shape, and structure. Furthermore, the potential biological effects of these AgNPs in treating myocardial infarction were evaluated.

2 Materials and methods

2.1 Preparation of aqueous extract

The newly harvested leaves of *S. oleracea* were rinsed with running water to eliminate any impurities and dust, followed by drying in the shade to create the powder. To create the leaf extract, 20 g of powder were placed into a 0.3 L conical flask with 0.2 L of distilled water. The mixture was heated on a magnetic stirrer at 65°C for 60 min. Subsequently, it was filtered using Whatman filter paper (No. 1), and the resulting leaf filtrate was utilized for the AgNPs' formulation.

2.2 Green formulation of AgNPs

To create the 1 mM AgNO₃ stock solution, the *S. oleracea* extract (80 mL) was combined with the AgNO₃ stock

solution (250 mL) and incubated at 25°C for 180 min. Then, a significant remarkable in color was observed in the reaction solution. The AgNPs' biosynthesis was confirmed by ultraviolet–visible spectroscopy (UV–Vis), field emission scanning electron microscopy (FE–SEM), Fourier-transform infrared spectroscopy (FT–IR), and energy-dispersive X-ray (EDX).

2.3 Chemical characterization of AgNPs

A UV–Vis spectrophotometric analysis was conducted to check the absorbance value of nanoparticles within the 200–800 nm range. The biogenic AgNP SPR was recorded using the UV–Vis spectrophotometer.

FE–SEM was utilized for the examination of the structure and makeup of AgNPs. The AgNPs' size distribution was depicted in a histogram by using ImageJ software.

The identification of the various functional groups accountable for the stabilization and reduction of the formulated AgNPs was accomplished through FT–IR analysis, utilizing the Cary 630 FT–IR model from Tokyo, Japan. The FT–IR analysis was conducted using the KBr technique, where a slice containing 0.3 g of formulated AgNPs mixed with KBr was created under high pressure.

2.4 Animals

Throughout this experimental study, 80 male BALB/c mice (38–40 g) each were employed. The animals were kept in a regulated environment between 20 and 24°C. It should be emphasized that all protocols followed in this research strictly complied with ethical standards for working with laboratory animals.

2.5 *In vivo* experimental design

- (1) Myocardial infarction + AgNPs (10 µg/kg).
- (2) Myocardial infarction + AgNPs (20 µg/kg).
- (3) Myocardial infarction group.
- (4) Control group.

After acclimating the mice to their environment, myocardial infarction was induced in the mice by administering ISO (85 mg/kg) dissolved in normal saline (1 mg/mL) subcutaneously for 2 consecutive days with a 24-h interval, following the methodology outlined in the study by Arozal

et al. [2]. (On the day after the injection, four animals experienced shedding, prompting immediate replacement.) The induction of myocardial infarction was established based on standard protocols. Subsequently, a selection of mice was anesthetized 48 h post-myocardial infarction, and samples of heart tissue from their left ventricle were analyzed using hematoxylin–eosin histochemical techniques. The presence of white areas signified necrotic injury resulting from the heart attack [2].

Following the final administration of ISO, the mice were subjected to anesthesia. The presence of ST segment depression or elevation in the animals was evaluated. On the 5th day, the mice were euthanized to evaluate the immunological and biochemical factors. The levels of IL-6, IL-1β, and TNF-α expression in the supernatant of homogenized left ventricles heart tissues were assessed using ELISA kits. The extent of myocardial cellular damage was determined by evaluating the levels of serum troponin and creatinine kinase isoenzyme. An ELISA was employed to measure the levels of serum creatinine kinase isoenzyme and troponin [2].

The RNA from the examined heart was extracted by the Qiasol kit (Qiagen) following the provided instructions. The isolated RNA purity and concentration were evaluated by a nanodrop spectrophotometer. The samples' optical absorption was assessed at 280 nm, and the concentration was determined based on the dilution factor in µL/ng. Subsequently, 1 ng/µL of RNA was prepared and utilized for cDNA synthesis. To achieve this objective, 10 µL of a cDNA synthesis kit was combined with 10 µL of RNA. The mixture was subsequently placed in a thermocycler and incubated for 10 min at 25°C, followed by 50 min at 60°C. Finally, the resulting cDNA was stored for qPCR analysis at –20°C. PCR was conducted to examine the gene replication rate. In this research, the control gene utilized was the beta-actin gene. The temperature program for PPAR/GAPDH gene amplification, including PPAR-γ/NF-κB/IκB-α/IKKα/β, PPAR-γ, and beta-actin, involved a series of steps. These steps consisted of primary denaturation for 4 min at 94°C, followed by secondary denaturation for 1 min at 94°C. The binding temperature was set for 1 min at 55°C, and primary synthesis occurred for 1 min at 52°C. This process was repeated for 40 cycles, encompassing steps 2–4, and concluded with the final synthesis. The temperature reached 52°C for 18 min. Subsequently, the graphs acquired were examined, and alterations in gene expression were determined through ΔΔCT analysis (based on the CT variance between the different intervention groups). The beta-actin gene expression was assessed using the following primer sequence: forward primer CCTGCACTGAATCAAGAGGTTGC and reverse primer CCATCAGAAGGACTTGCTGGCT [2].

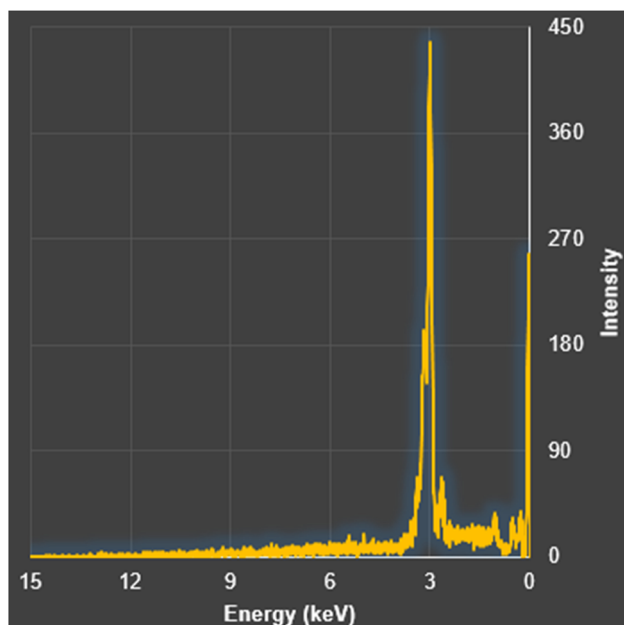


Figure 1: EDX analysis of AgNPs green mediated by *S. oleracea*.

2.6 Statistical analysis

In this study, the data's normality was determined through Minitab-21. Subsequently, any non-normal data were normalized. The data variance test was conducted using SPSS-22, and visual representations were created through Excel software.

3 Results and discussion

3.1 Chemical characterization

EDX analysis is the practical method for elemental screening of nanomaterials. The EDX diagram and quantitative results of the elemental table of AgNPs green mediated by *S. oleracea* of nanoparticles are revealed in Figure 1 and Table 1. The energy signals at 3.02 and 2.64 keV are designated for Ag L β and Ag L α , respectively. The presence of signals at 0.52 (O

La) and 0.27 (for C La) confirms the secondary metabolites connection from the extract to the synthetic AgNP surface [2,25]. Arozal et al. have reported comparable signals for AgNPs produced with *Salvia leriifolia* [2].

FT-IR is an analytical technique of great reliability that identifies and exhibits functional groups, chemical bonds, chemical structures, elements, and bonding arrangements of molecules [9,39]. Characterization of AgNPs using FT-IR is conducted to determine the molecules responsible for coating and stabilizing, as well as to observe the reduction of silver ions [20]. The reduction or capping in the green synthesis of AgNPs [30] can be attributed to the presence of amide and carboxylic functional groups, as indicated by the FT-IR spectra. The leaf extract of *Catharanthus roseus* was utilized to synthesize AgNPs with a green approach. The synthesized AgNPs exhibited significant peaks at 1,208, 1,084, 1,706, 2,073, and 2,401 cm^{-1} , indicating the existence of various functional groups. These functional groups include the secondary amine (N-H) group, primary amine (N-H) group, phenyl ring, alcohol and amide groups, ketone group (C=O), alkynes group (RC=CH), and carboxylic acid group (O-H), respectively [9]. The FT-IR spectrum of nanoparticles synthesized using *Tectona grandis* seeds' extract displayed peaks at 1,038, 1,508, 1,643, and 1,745 cm^{-1} , which corresponded to the stretching vibrations of different chemical bonds such as amine bond, nitro compounds, proteins' amide bond, and carboxylic acid or ester, as reported in the study [40].

The metal-oxygen bond is associated with bands below 700 cm^{-1} in FT-IR analysis. In Figure 2 of the FT-IR spectrum of AgNPs, the Ag-O bond is represented by bands at 457 and 576 cm^{-1} . The additional peaks at 1,038, 1,323–1,630, 2,940, and 3,269 cm^{-1} correspond to the carbonyl (CO), C=C, CO₂, and hydroxyl (OH) organic functional groups of *S. oleracea*, which serve as the reducing agent during the synthesis process.

The mixture of plant extract and silver nitrate salt was combined and left to incubate for 180 min. Throughout this period, a noticeable alteration in color occurred within the reaction mixture. The initial yellow-orange hue of the solution transformed into a deep brown shade, thereby

Table 1: Quantitative results of the elemental table of AgNPs green mediated by *S. oleracea*

Elt	Line	Int	Error	K	Kr	W%	A%	ZAF	Formula	Ox%	Pk/Bg	Class	LConf	HConf	Cat#
C	Ka	328.4	5.5490	0.3884	0.2392	36.23	61.33	0.6604		0.00	33.16	A	34.97	37.49	0.00
N	Ka	18.2	5.5490	0.0277	0.0171	7.56	10.97	0.2261		0.00	7.47	A	6.44	8.67	0.00
O	Ka	69.1	5.5490	0.0470	0.0289	15.81	20.09	0.1830		0.00	16.09	A	14.61	17.00	0.00
Ag	La	496.6	4.5305	0.5369	0.3307	40.41	7.62	0.8184		0.00	18.30	A	39.27	41.55	0.00
				1.0000	0.6160	100.00	100.00			0.00					0.00

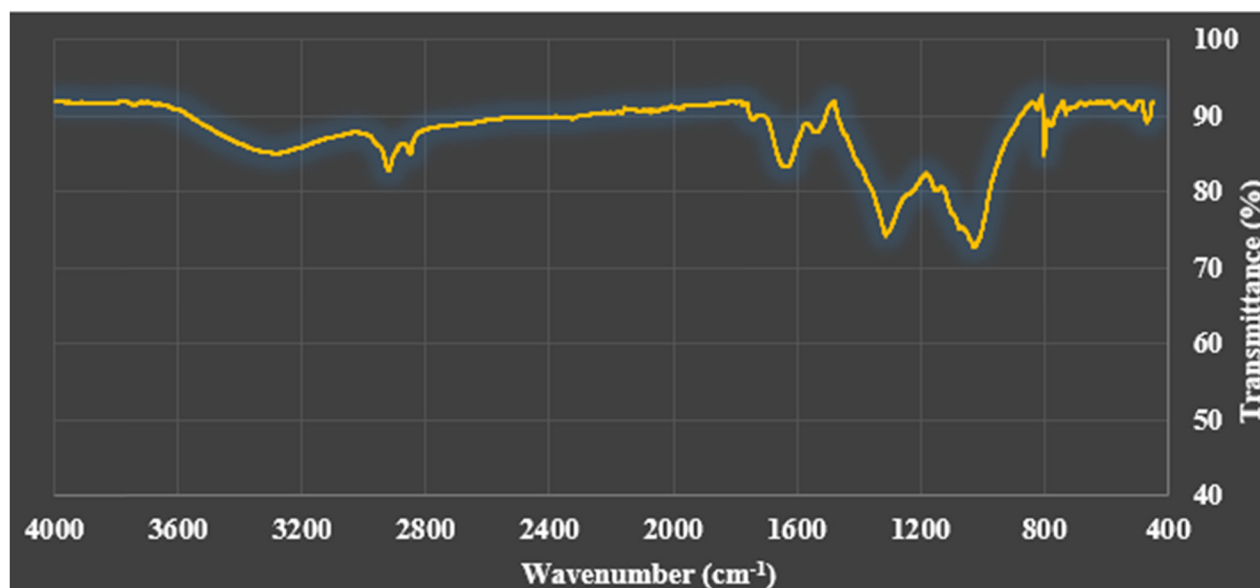


Figure 2: FT-IR analysis of AgNPs green mediated by *S. oleracea*.

confirming the occurrence of phytosynthesis in the production of AgNPs. The alteration in color occurred as a result of the SPR activity exhibited by the nanoparticles [2,5]. The color intensity is dictated by the quantity of electrons liberated during the conversion of NO_3 to NO_2 , leading to the Ag^+ reduction to metallic ions (Ag^0) [14,15]. The research we conducted was backed by the results from Refs. [2,5], which mirrored our findings regarding the visual alteration of the solution's color. Further investigation into the reaction solution color change was conducted by analyzing the AgNPs UV-Vis spectrum. The confirmation of AgNP formation was established by the presence of the SPR peak at 411 nm in this study.

The synthesis of AgNPs involves a colorful reaction that exhibits intense and distinct absorption bands within the visible spectrum, typically ranging from 400 to 500 nm [26]. Three different concentrations of pure curcumin were used to synthesize curcumin-loaded AgNPs: 0.25 g (C2), 0.1 g (C1), and 0.005 g (C0). The absorbance spectra observed were at 445, 428, and 427 nm for C2, C1, and C0, respectively [27]. The UV-Vis analysis of green-synthesized nanoparticles loaded with *Salvia spinosa*-grown extract revealed a wide bell-shaped spectrum curve [28]. In numerous studies, UV-Vis spectroscopy has been utilized to measure the change in reaction color and the decrease in silver ions [28–30] (Figure 3).

One technique utilized to characterize metal nanoparticles involves examining an electron microscope (FE-SEM) image, which is useful for analyzing the morphology of the produced NPs. The FE-SEM image captured from AgNPs

under the specified ideal parameters reveals the production of spherical nanomaterials (Figure 4). The particles that were generated had a size of 10–50 nm. On average, the nanoparticles that were synthesized had a size between 15 and 30 nm. In terms of their morphology, the nanoparticles exhibited crystalline geometric and uniform shapes. Additionally, due to the lengthy waiting time for analysis, the AgNPs tended to agglomerate to some extent.

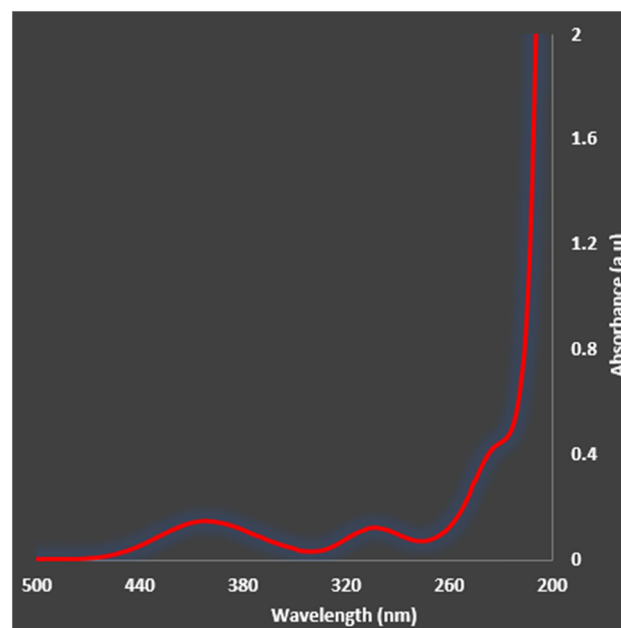


Figure 3: UV-Vis analysis of AgNPs green mediated by *S. oleracea*.

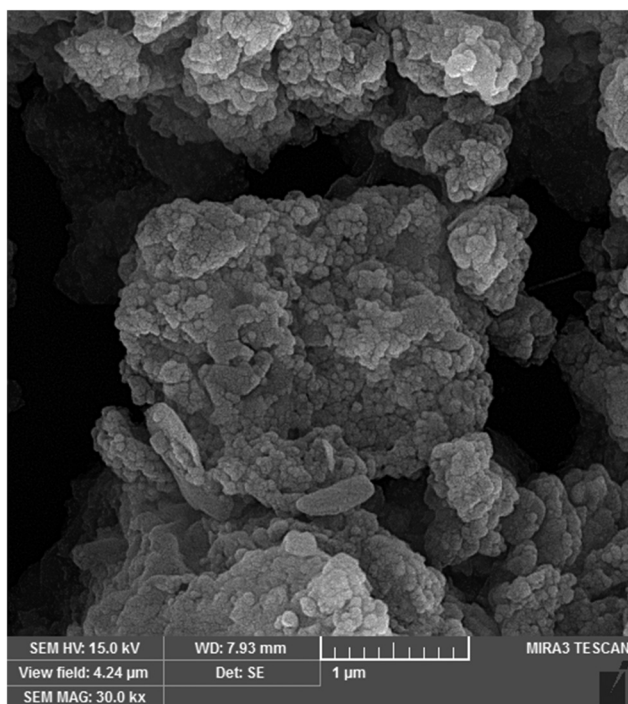


Figure 4: FE-SEM image of AgNPs green mediated by *S. oleracea*.

3.2 Cardioprotective effects of AgNPs green mediated by *S. oleracea*

In a recent study, mice were administered ISO to induce myocardial infarction. High doses of ISO rapidly elevate the myocardial load, leading to myocardial dysfunction. The morphological and pathophysiological alterations caused by ISO in mice closely resemble those observed in human myocardial infarction. Free radical-enhanced generation in myocardial infarction elevates the activity of the mitogen-activated protein kinase (MAPK) signaling pathway, consisting of three subfamilies namely p38, JNK, and ERK. Activation of this pathway upregulates κ B-NF, resulting in heightened production of inflammatory cytokines and ultimately contributing to myocardial damage [31,32]. To date, extensive research has been conducted on the ERK signaling pathway, which is instrumental in governing cellular death, growth, and survival, as well as the immune response associated with inflammation [31]. Although p38 MAPK and JNK are associated with apoptosis, ERK is crucial in promoting cell survival and reducing the risk of myocardial infarction [32]. Multiple research has revealed the κ B-NF and MAPK pathways' involvement in myocardial hypertrophy, heart failure, and blood pressure regulation. Various research findings have suggested that inhibiting MAPK can result in the activation of 2-Nrf, which is crucial in regulating the expression of antioxidant and detoxification enzymes during the second step [31–33].

The research presented a green formulation of AgNPs green synthesized with *S. oleracea*. Various spectroscopic techniques were employed to characterize the AgNPs, and their effectiveness in treating myocardial infarction was investigated.

In the current research, the protective effects of nanoparticles produced from *S. oleracea* against myocardial damage were investigated by inducing a myocardial infarction model in mice using ISO. Furthermore, the expression levels of PPAR- γ /NF- κ B/I κ B- α /IKK α / β and PPAR- γ or MAPK signaling pathway in the experimental groups were assessed to understand the mechanism of the treatment applied (refer to Figure 5). The green-mediated *S. oleracea* AgNPs led to a reduction in the levels of p-IKK α /IKK α / β , p-I κ B/I κ B α , and p-NF- κ B p65/NF- κ B p65, as well as a decrease in PPAR/GAPDH. Furthermore, the green-mediated AgNPs derived from *S. oleracea* exhibited a significant reduction ($P \leq 0.05$) in the mRNA levels of IL-6, TNF- α , and IL-1 β , as well as the presence of CD68+ cells, when compared to the untreated group (Figures 6–8). The mice under study exhibited a myocardial infarction model induced by ISO, as evidenced by the substantial collagen deposition and extensive damage to the myocardial tissue. Moreover, the expression of MAPK was elevated, further confirming the effectiveness of the model. According to recent research, it has been suggested that numerous signaling pathways, including the proteins of the MAPK pathway, undergo alterations in myocardial damage induced by ISO [34]. Recent research has demonstrated the effectiveness of ISO in inducing an increase in MAPK levels. The MAPK pathway has a crucial role in regulating the genes' expression associated with apoptosis, including Bax and Bcl-2. These genes are apoptotic signaling pathway vital components and activate within the cell upon receiving extracellular signals. Furthermore, the occurrence of myocardial infarction leads to inflammatory cytokines secretion and enhances the activity of MAPK P38 [35]. *S. oleracea*-synthesized nanoparticles exhibit promising potential in the myocardial damage treatment resulting from ISO consumption. The antioxidant properties of these nanoparticles, along with their compounds, demonstrate a notable impact on the inhibition of DPPH free radicals. Enhancing the body's immune system through enhancing antioxidant levels unquestionably shields individuals from numerous long-term illnesses. According to Martinez *et al.*, antioxidants can decrease the risk of heart failure by influencing MAPK and NF- κ B signaling pathways [36]. Hence, the potential impact of *S. oleracea*-derived nanoparticles on diminishing MAPK expression could be attributed to their antioxidative characteristics.

It has been confirmed that oxidative stress can trigger the activation of NF- κ B, a key transcription factor activated in response to oxidative stress. This signaling pathway is

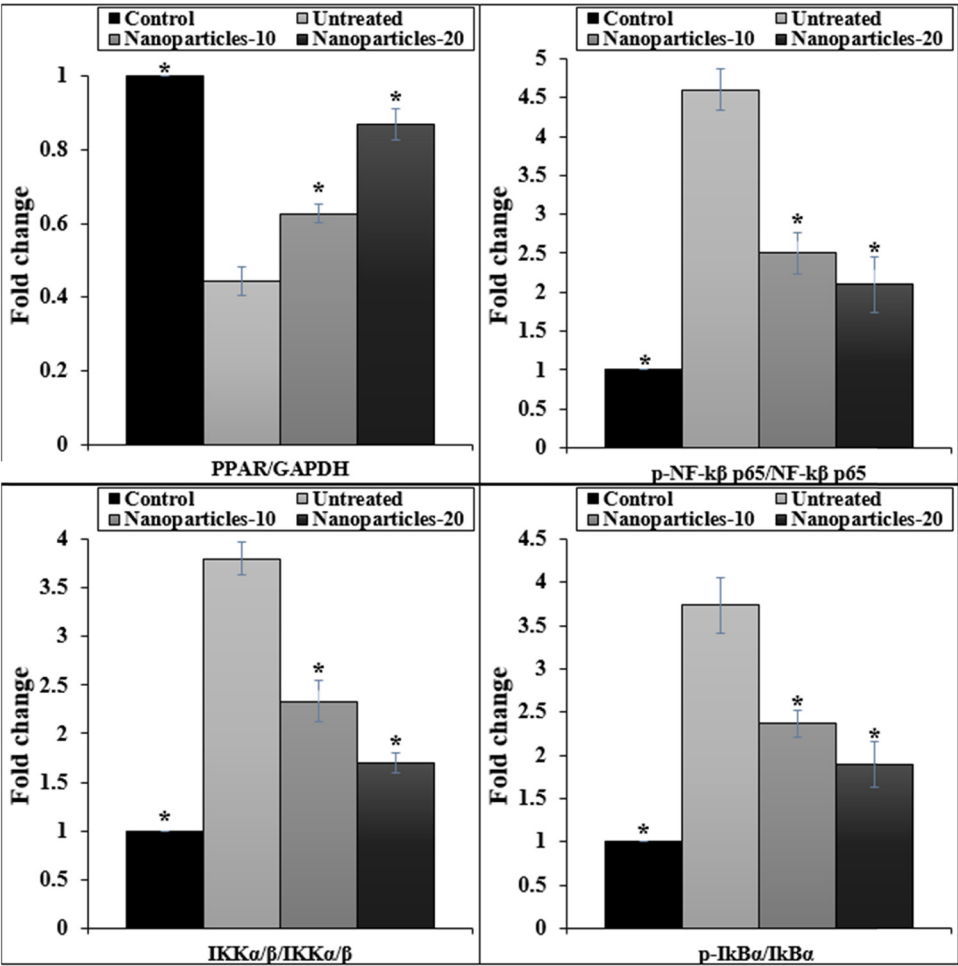


Figure 5: The activity of AgNPs on PPAR/GAPDH, p-NF-kB p65/NF-kB p65, p-IkBα/IkBα, and p-IKKα/β/IKKα/β (fold change).

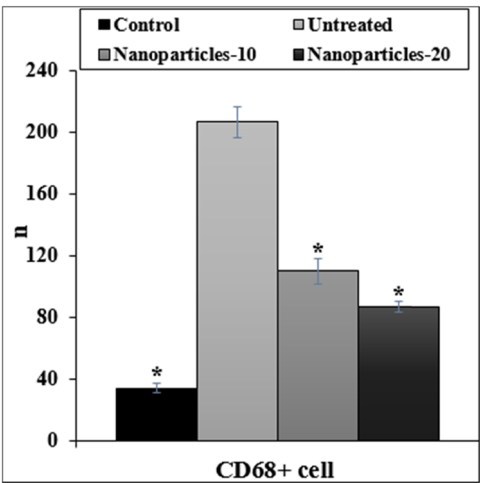


Figure 6: The activity of AgNPs on the CD68⁺ cell.

crucial for cell proliferation and differentiation, ultimately leading to cardioprotective benefits. In addition to the

cardioprotective impact of AgNPs, NF-κB is involved in initial inflammatory reactions and can stimulate the production of various inflammatory cytokines including TNF-α, IL-1, and IL-6. Furthermore, NF-κB seems to have negative effects on myocytes [33,34]. Previous research has demonstrated that the activation of NF-κB plays a crucial role in developing doxorubicin-induced cardiotoxicity [2,34]. In the current investigation, the administration of ISO was linked to an elevation in the expression of NF-κB protein. Notably, the simultaneous use of AgNP resulted in a reduction in NF-κB expression, indicating that the formulation of AgNP has a mitigating impact on the inflammatory response derived from NF-κB. Likewise, a recent laboratory study utilizing AgNPs bio-capped with macroalgae demonstrated an anti-inflammatory characteristic [2].

The latest research revealed that the AgNPs synthesized using *S. oleracea* led to a reduction in cardiac troponin-1, cTn-T, ST segment deviation in MI mice, as well as the heart wet weight/body weight ratio as compared to the control group (Figures 9–11). In agreement with our study,

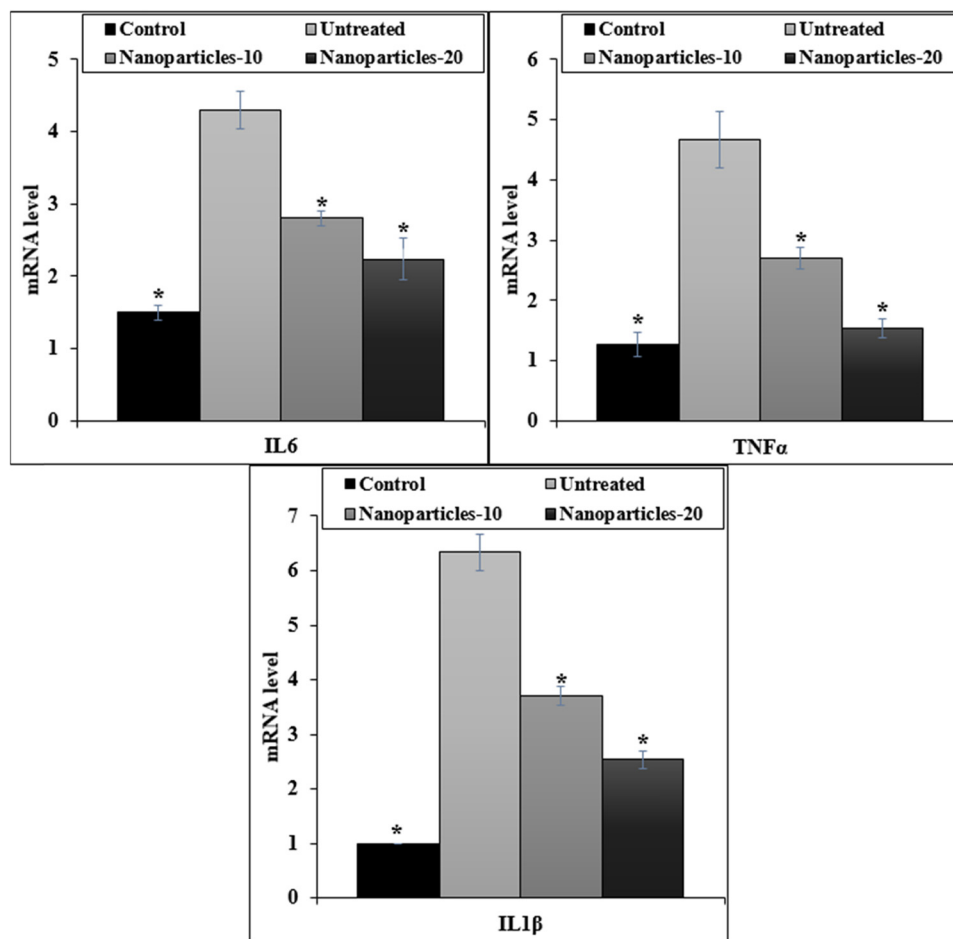


Figure 7: The activity of AgNPs on the IL-1β, TNF-α, and IL-6 mRNA levels.

Arozal et al. indicated the cardioprotective efficacies of AgNPs on myocardial infarction by reducing the cardiac troponin-1, cTn-T, and ST segment deviation in MI mice [2].

It remains uncertain as to the precise mechanism by which AgNPs raise the ROS generation, although they do create a pro-oxidant environment. Several hypotheses propose a connection between the release and buildup of intracellular Ag⁺ and the heightened ROS production. However, recent data suggest that AgNPs, not the ions they release, are responsible for generating ROS. There is a wealth of evidence showing the harmful effects of AgNPs on different bodily systems [37,38]. AgNPs have been demonstrated to cause damage to various organs and tissues, including the vasculature, kidneys, spleen, lungs, bone marrow, liver, sperm cells, and skin. Research suggests that these nanoparticles disrupt the fusion of lysosomes and autophagosomes through defective ubiquitination at the subcellular level [9]. Future research focusing on the AgNPs' genotoxic effects and their possible involvement in cancer is currently a topic of interest, as

indicated by various studies [38]. It is intriguing to note that while certain studies argue that these particles primarily avoid causing harm to the blood–brain barrier (BBB), other findings indicate that the administration of AgNP can actually change the BBB's permeability. This discovery opens up an intriguing possibility for future applications [37,38]. AgNPs have found extensive applications in various fields such as medical advancements, environmental protection, food preservation, and domestic utilities, owing to their exceptional characteristics. Many reviews and chapters have been dedicated to discussing the various applications of AgNPs [39–42]. These publications particularly emphasize the wide range of biomedical and biological uses of AgNPs, such as their effectiveness in combating viruses, fungi, bacteria, cancer, inflammation, and angiogenesis [39–42]. Arozal et al. [2] investigated the effects of AgNPs on the ISO-induced myocardial infarction model in rats, comparing their anti-inflammatory and antioxidant properties to those of the conventional silver form [2]. In addition, the examination of AgNPs will be conducted among the

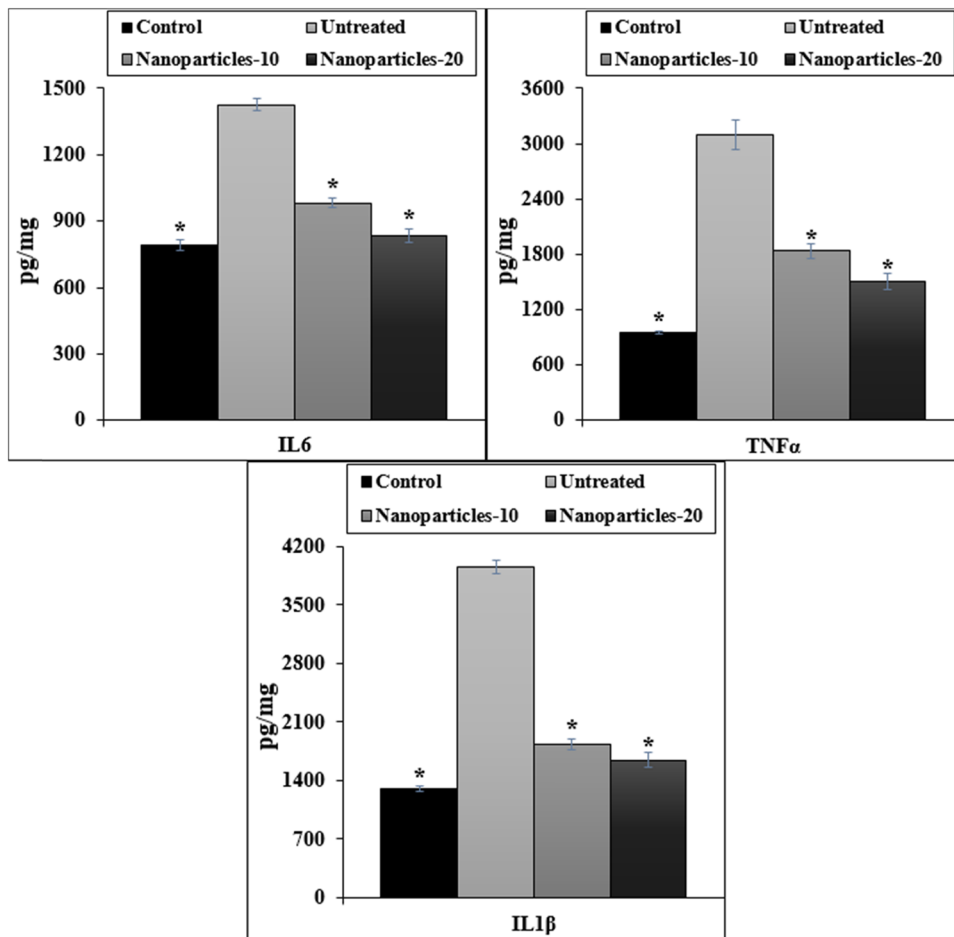


Figure 8: The activity of AgNPs on the IL-1 β , TNF- α , and IL-6 concentration (pg/mg).

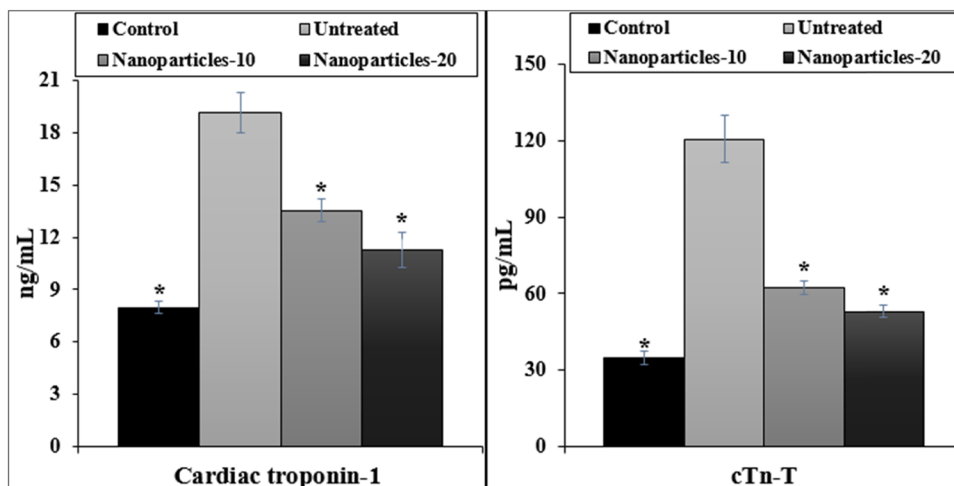


Figure 9: The activity of AgNPs on the concentrations of cardiac troponin-1 (ng/mL) and cTn-T (pg/mL).

treatment groups due to their potential impact on mitochondria biogenesis. The AgNPs' safety profiles included the evaluation of kidney and liver functions. Furthermore, the

study investigated the dysregulation of mitochondria caused by ISO [2]. After a 14-day pretreatment with AgNPs, the mRNA expression levels of PGC-1 α and TFAM were

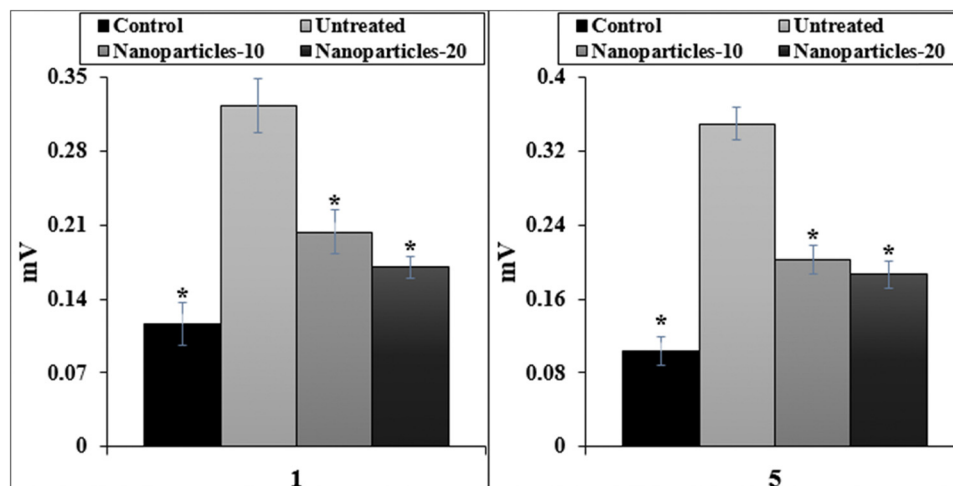


Figure 10: The activity of AgNPs on MI mice ST segment deviation (mV).

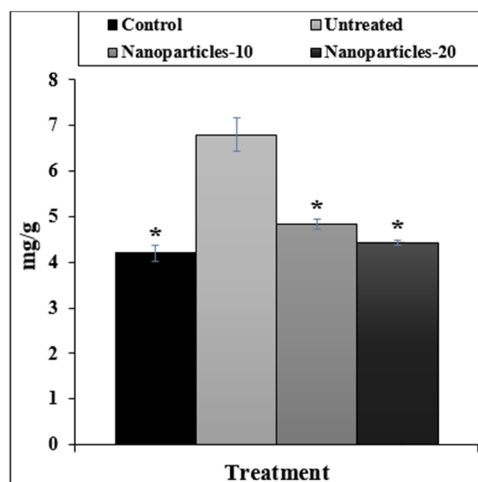


Figure 11: The activity of AgNPs on heart wet weight/body weight ratio (mg/g).

significantly higher compared to other groups. Interestingly, the mRNAs' expression levels in the ISO group were similar to those in the normal group [2]. AgNPs demonstrate unique impacts, suggesting that AgNPs can specifically penetrate the mitochondria or nucleus to induce the PGC-1 α and TFAM expression, ultimately safeguarding cardiac cells [2]. Contrary to the assertions made in numerous published articles, exposure to AgNPs has the potential to induce mitochondrial damage in cells. This damage encompasses swelling, mitochondrial membrane potentials disruption, and apoptosis triggered through the mitochondrial pathway [43]. The formulation of AgNPs created by Arozal *et al.* [2] exhibited beneficial effects due to the eco-friendly synthesis method involving alginate. The study demonstrated a correlation between the ISO administration in rats and myocardial

injury by analyzing creatine kinase-MB (CK-MB) and lactate dehydrogenase activities, which are cardiac enzyme leakage indicators [2]. Upon comparison of the AgNP group with the ISO group, a notable reduction in CK-MB activity was observed, indicating that Ag offers protection on myocardial damage. Although both AgNPs enhanced cardiac enzyme markers, it was only AgNPs that could effectively reverse the histological changes in the myocardium induced by ISO [2].

4 Conclusion

Our team has successfully created an advanced medication for cardioprotection by utilizing AgNPs infused with *S. oleracea*. This innovative treatment aims to address ISO-induced myocardial infarction in mice, with a specific focus on the PPAR- γ /NF- κ B pathway. The region of 400–700 cm^{-1} exhibited vibrational bands for Ag–O bonds, as revealed by the FT-IR spectroscopy. Additionally, the FE-SEM image displayed a spherical morphology (below 50 nm). AgNPs have been shown to lower the pro-inflammatory cytokine levels in the mice hearts with myocardial infarction. Additionally, they have been found to effectively inhibit the myocardial injury markers levels, decrease mortality rates, and improve ventricular wall infarction. The positive effects of AgNPs may be related to the gene expression normalization related to PPAR- γ /NF- κ B/I κ B- α /IKK α / β and PPAR- γ phosphorylation.

Funding information: Authors state no funding.

Author contributions: All authors have the same role in the conceptualization, investigation, acquisition, formal

analysis, data curation, supervision, project administration, methodology, validation, resources, writing – original draft, and writing – review & editing.

Conflict of interest: There is no any conflict of interest.

Ethical approval: The experiments were performed according to the ethical guidelines of the International Association for the Study of Humans.

Data availability statement: The datasets generated during and/or analyzed during the current study are available from the corresponding author upon reasonable request.

References

- [1] Scafa Udriște A, Burdușel AC, Niculescu AG, Rădulescu M, Grumezescu AM. Metal-based nanoparticles for cardiovascular diseases. *Int J Mol Sci.* 2024 Jan;25(2):1001.
- [2] Arozal W, Monayo ER, Barinda AJ, Perkasa DP, Soetikno V, Nafrialdi N, et al. Protective effects of silver nanoparticles in isoproterenol-induced myocardial infarction in rats. *Front Med (Lausanne).* 2022 Aug;9:867497.
- [3] Sun R, Wang X, Nie Y, Hu A, Liu H, Zhang K, et al. Targeted trapping of endogenous endothelial progenitor cells for myocardial ischemic injury repair through neutrophil-mediated SPIO nanoparticle-conjugated CD34 antibody delivery and imaging. *Acta Biomater.* 2022;146:421–33.
- [4] Sosnovik DE, Nahrendorf M, Deliolanis N, Novikov M, Aikawa E, Josephson L, et al. Fluorescence tomography and magnetic resonance imaging of myocardial macrophage infiltration in infarcted myocardium in vivo. *Circulation.* 2007;115:1384–91.
- [5] Lin CX, Yang SY, Gu JL, Meng J, Xu HY, Cao JM. The acute toxic effects of silver nanoparticles on myocardial transmembrane potential, I (Na) and I(K1) channels and heart rhythm in mice. *Nanotoxicology.* 2017;11:827–37.
- [6] Shen Y, Gong S, Li J, Wang Y, Zhang X, Zheng H, et al. Co-loading antioxidant N-acetylcysteine attenuates cytotoxicity of iron oxide nanoparticles in hypoxia/reoxygenation cardiomyocytes. *Int J Nanomed.* 2019;14:6103–15.
- [7] Danila D, Johnson E, Kee P. CT imaging of myocardial scars with collagen-targeting gold nanoparticles. *Nanomed Nanotechnol Biol Med.* 2013;9:1067–76.
- [8] Bakir EM, Younis NS, Mohamed ME, El Semaary NA. Cyanobacteria as nanogold factories: Chemical and anti-myocardial infarction properties of gold nanoparticles synthesized by *Lyngbya majuscula*. *Mar Drugs.* 2018;16:217.
- [9] Ferdous Z, Al-Salam S, Greish YE, Ali BH, Nemmar A. Pulmonary exposure to silver nanoparticles impairs cardiovascular homeostasis: Effects of coating, dose and time. *Toxicol Appl Pharmacol.* 2019;367:36–50.
- [10] Yilmaz A, Dengler MA, van der Kuip H, Yildiz H, Rösch S, Klumpp S, et al. Imaging of myocardial infarction using ultrasmall superparamagnetic iron oxide nanoparticles: A human study using a multi-parametric cardiovascular magnetic resonance imaging approach. *Eur Heart J.* 2013;34:462–75.
- [11] Merinopoulos I, Gunawardena T, Stirrat C, Cameron D, Eccleshall SC, Dweck MR, et al. Diagnostic applications of ultrasmall superparamagnetic particles of iron oxide for imaging myocardial and vascular inflammation. *JACC: Cardiovasc Imaging.* 2021;14:1249–64.
- [12] Zheng H, You J, Yao X, Lu Q, Guo W, Shen Y. Superparamagnetic iron oxide nanoparticles promote ferroptosis of ischemic cardiomyocytes. *J Cell Mol Med.* 2020;24:11030–3.
- [13] Sim W, Barnard R, Blaskovich MAT, Ziora Z. Antimicrobial silver in medicinal and consumer applications: A patent review of the past decade (2007–2017). *Antibiotics.* 2018;7:93.
- [14] Ajdary M, Negahdary M, Chelongar R, Zadeh S. The antioxidant effects of silver, gold, and zinc oxide nanoparticles on male mice in vivo condition. *Adv Biomed Res.* 2015;4:69.
- [15] Alkhalaf MI, Hussein RH, Hamza A. Green synthesis of silver nanoparticles by *Nigella sativa* extract alleviates diabetic neuropathy through anti-inflammatory and antioxidant effects. *Saudi J Biol Sci.* 2020;27:2410–9.
- [16] Docea AO, Calina D, Buga AM, Zlatian O, Paoliello MMB, Mogosanu GD, et al. The effect of silver nanoparticles on antioxidant/pro-oxidant balance in a murine model. *Int J Mol Sci.* 2020;21:1233.
- [17] Asgharzadeh F, Hashemzadeh A, Yaghoubi A, Avan A, Nazari SE, Soleimanpour S, et al. Therapeutic effects of silver nanoparticle containing sulfasalazine on DSS-induced colitis model. *J Drug Deliv Sci Technol.* 2021;61:102133.
- [18] Yang Y, Guo L, Wang Z, Liu P, Liu X, Ding J, et al. Targeted silver nanoparticles for rheumatoid arthritis therapy via macrophage apoptosis and re-polarization. *Biomaterials.* 2021;264:120390.
- [19] Begum Q, Mahboob T. Silver nanoparticles protects streptozotocin-induced hepatotoxicity: A biochemical and histopathological approach. *Int J Nano Res.* 2020;4:1–9.
- [20] Prasannaraj G, Venkatachalam P. Hepatoprotective effect of engineered silver nanoparticles coated bioactive compounds against diethylnitrosamine induced hepatocarcinogenesis in experimental mice. *J Photochem Photobiol B Biol.* 2017;167:309–20.
- [21] Kazmi SAR, Qureshi MZ, Sadia, Alhewairini SS, Ali S, Khurshid S, et al. Minocycline-derived silver nanoparticles for assessment of their antidiabetic potential against alloxan-induced diabetic mice. *Pharmaceutics.* 2021;13:1678.
- [22] Li L, Bi Z, Hu Y, Sun L, Song Y, Chen S, et al. Silver nanoparticles and silver ions cause inflammatory response through induction of cell necrosis and the release of mitochondria in vivo and in vitro. *Cell Biol Toxicol.* 2021;37:177–91.
- [23] Simon-Deckers A, Gouget B, Mayne-L'Hermite M, Herlin-Boime N, Reynaud C, Carrière M. In vitro investigation of oxide nanoparticle and carbon nanotube toxicity and intracellular accumulation in A549 human pneumocytes. *Toxicology.* 2008;253:137–46.
- [24] Skalska J, Dąbrowska-Bouta B, Frontczak-Baniewicz M, Sulkowski G, Strużyńska LA. Low dose of nanoparticulate silver induces mitochondrial dysfunction and autophagy in adult rat brain. *Neurotox Res.* 2020;38:650–64.
- [25] (a) Goudarzi M, Mir N, Mousavi-Kamazani M, Bagheri S, Salavati-Niasari M. Biosynthesis and characterization of silver nanoparticles prepared from two novel natural precursors by facile thermal decomposition methods. *Sci Rep.* 2016;6:32539; (b) Gowramma B, Keerthi U, Rafi M, Muralidhara Rao D. Biogenic silver nanoparticles

- production and characterization from native stain of *Corynebacterium* species and its antimicrobial activity. 3 Biotech. 2015;5:195–201.
- [26] Noah N. Green synthesis: characterization and application of silver and gold nanoparticles. Green Synth Charact Appl Nanopart. 2019;53:111–35.
- [27] Khan MJ, Shameli K, Sazili AQ, Selamat J, Kumari S. Rapid green synthesis and characterization of silver nanoparticles arbitrated by curcumin in an alkaline medium. Molecules. 2019;24:719.
- [28] Pirtarighat S, Ghannadnia M, Baghshahi S. Green synthesis of silver nanoparticles using the plant extract of *Salvia spinosa* grown in vitro and their antibacterial activity assessment. J Nanostruct Chem. 2019;9:1–9.
- [29] Gudikandula K, Maringanti SC. Synthesis of silver nanoparticles by chemical and biological methods and their antimicrobial properties. J Exp Nanosci. 2016;11(9):714–21.
- [30] Ahmed S, Saifullah Ahmad M, Swami BL, Ikram S. Green synthesis of silver nanoparticles using *Azadirachta indica* aqueous leaf extract. J Rad Res App Sci. 2016;9:1–7.
- [31] Ren G, Cui Y, Li W, Li F, Han X. Research on cardioprotective effect of irbesartan in rats with myocardial ischemia-reperfusion injury through MAPK-ERK signaling pathway. Eur Rev Med Pharmacol Sci. 2019;23(12):5487–94.
- [32] Liu K, Wang F, Wang S, Li W-N, Ye Q. Mangiferin attenuates myocardial ischemia-reperfusion injury via MAPK/Nrf-2/HO-1/NF-κB in vitro and in vivo. Oxid Med Cell Longev. 2019;2019:7285434.
- [33] Bao W, Hu E, Tao L, Boyce R, Mirabile R, Thudium DT, et al. Inhibition of Rho-kinase protects the heart against ischemia/reperfusion injury. Cardiovasc Res. 2004;61(3):548–58.
- [34] Fakhri F, Shakeryan S, Fakhri S, Alizadeh A. The effect of 6 weeks of high intensity interval training (HIIT) with nano-curcumin supplementation on factors related to cardiovascular disease in inactive overweight girls. Feyz Med Sci J. 2020;24(2):181–9.
- [35] Krishnamurthy P, Rajasingh J, Lambers E, Qin G, Losordo DW, Kishore R. IL-10 inhibits inflammation and attenuates left ventricular remodeling after myocardial infarction via activation of STAT3 and suppression of HuR. Circ Res. 2009;104(2):e9–18.
- [36] Martinez PF, Bonomo C, Guizoni DM, Junior SAO, Damatto RL, Cezar MD, et al. Modulation of MAPK and NF-κB signaling pathways by antioxidant therapy in skeletal muscle of heart failure rats. Cell Physiol Biochem. 2016;39(1):371–84.
- [37] Karademir F, Ayhan F. Antimicrobial surface functionality of PEG coated and AgNPs immobilized extracorporeal biomaterials. Biointerface Res Appl Chem. 2021;12:1039–52.
- [38] Dixon K, Bonon R, Ivander F, Ale Ebrahim S, Namdar K, Shayegannia M, et al. Using machine learning and silver nanoparticle-based surface-enhanced raman spectroscopy for classification of cardiovascular disease biomarkers. ACS Appl Nano Mater. 2023;6:15385–96.
- [39] Zhang X-F, Liu Z-G, Shen W, Gurunathan S. Silver nanoparticles: Synthesis, characterization, properties, applications, and therapeutic approaches. Int J Mol Sci. 2016;17:1534.
- [40] Gherasim O, Puiu RA, Bîrcă AC, Burduşel AC, Grumezescu AM. An updated review on silver nanoparticles in biomedicine. Nanomaterials. 2020;10:2318.
- [41] Kumawat M, Madhyastha H, Singh M, Revaprasadu N, Srinivas SP, Daima HK. Double functionalized haemocompatible silver nanoparticles control cell inflammatory homeostasis. PLoS ONE. 2022;17:e0276296.
- [42] Almatroudi A. Silver nanoparticles: Synthesis, characterisation and biomedical applications. Open Life Sci. 2020;15:819–39.
- [43] Badi'Ah HI, Seede F, Supriyanto G, Zaidan AH. Synthesis of silver nanoparticles and the development in analysis method. IOP Conf Ser: Earth Environ Sci. 2019;217:012005. IOP Publishing.